

# Thrombus formation: direct real-time observation and digital analysis of thrombus assembly in a living mouse by confocal and widefield intravital microscopy

A. CELI,<sup>1</sup> G. MERRILL-SKOLOFF, P. GROSS, S. FALATI, D. S. SIM, R. FLAUMENHAFT, B. C. FURIE and B. FURIE

Center for Hemostasis and Thrombosis Research, Beth Israel Deaconess Medical Center and Harvard Medical School, Boston, MA, USA

**Summary.** We have developed novel instrumentation using confocal and widefield microscopy to image and analyze thrombus formation in real time in the microcirculation of a living mouse. This system provides high-speed, near-simultaneous acquisition of images of multiple fluorescent probes and a brightfield channel, and supports laser-induced injury through the microscope optics. Although this imaging facility requires interface of multiple hardware components, the primary challenge in vascular imaging is careful experimental design and interpretation. This system has been used to localize tissue factor during thrombus formation, to observe defects in thrombus assembly in genetically altered mice, to study the kinetics of platelet activation and P-selectin expression following vascular injury, to analyze leukocyte rolling on arterial thrombi, to generate three-dimensional models of thrombi, and to analyze the effect of antithrombotic agents *in vivo*.

**Keywords:** confocal, intravital microscopy, molecular imaging, platelets, tissue factor, thrombus

## Introduction

Blood coagulation is a complex and finely regulated host defense mechanism [1]. Perturbations of this system are well-recognized causes of diseases such as thrombosis, atherosclerosis, and hemorrhagic disorders. Our current models of the basic mechanisms of blood coagulation are mostly based on extrapolations from *in vitro* experiments. However, our understanding of these phenomena would greatly benefit from the availability of tools for *in vivo* observation and analysis. In recent years, a number of technological breakthroughs in dis-

parate fields have converged to offer the possibility to address old questions with new tools. The availability of techniques to manipulate the genome in mice, thereby generating transgenic, knockout and knock-in mouse strains, allows identification of the role of a single gene and its product in specific physiologic phenomena. This has in turn prompted the development of mouse models of human disease in order to take advantage of these genetically engineered animals to study the role of single proteins in different pathologic conditions, including thrombosis [2]. Intravital microscopy, the microscopic analysis of living cells, has been widely used and extended to the study of the microcirculation by many investigators [3]. However, only recently have advances in microscopy technology made possible the development of a confocal microscope that is capable, through the use of Nipkow disk technology, of acquiring images compatible with video-frame rates [4]. Finally, the digital revolution has fostered the development of relatively inexpensive but powerful computer workstations that can handle rapid data collection and quickly store massive amounts of image information in digital format. We took advantage of the availability of these tools to design and assemble instrumentation that combines high-speed widefield and confocal fluorescence microscopy with a nitrogen laser that delivers an injury via the microscope optics to the vascular wall. This instrument provides the ability to image thrombus formation in real time in the microcirculation of a living mouse. We used fluorescently labeled antibodies directed against cell-specific or soluble antigens to study the role of specific cell populations and proteins in thrombus formation in wild-type mice and in mice with a spectrum of genetic modifications. To facilitate access to this technology and its potential for furthering basic and applied research in blood coagulation and vascular biology, we provide here a full description of the components of this system and the methods that we have used to generate and rigorously analyze data. Since both the hardware, software and user applications continue to evolve rapidly, the description that follows is current, but likely to change with continued improvements.

## Real-time *in vivo* imaging

Our system involves the imaging of the cremaster muscle microcirculation in a living mouse. Although other vascular windows have been used in our laboratory, including the

Correspondence: Dr Bruce Furie, Center for Hemostasis and Thrombosis Research, Research East 319, Beth Israel Deaconess Medical Center, 330 Brookline Ave, Boston MA 02215, USA.

Tel.: + 617 667 0620; fax: + 617 975 5505.

e-mail: bfurie@caregroup.harvard.edu

<sup>1</sup>Present address: Laboratorio di Biologia Cellulare Respiratoria, Dipartimento Cardiotoracico, Università di Pisa, Pisa, Italy.

Received 01 October 2002, accepted 10 October 2002

mesenteric microcirculation and the ear microcirculation, the cremaster muscle offers excellent blood vessel images because it is thin and transparent, contains many arterioles and venuoles, and permits a stable preparation for multiple hours of study. Wild-type mice and genetically altered mice are routinely employed, and thus provide important information about the role of particular gene products in thrombus formation. We employ a laser-induced injury model [5]. Although many other injury models have been adapted to experiments in the mouse [2], the laser injury is temporally and spatially defined and its magnitude adjustable. Confocal imaging employs laser excitation, a high-speed confocal scanner using Nipkow disk technology, and capture of intensified images on a high-speed digital CCD camera. Widefield imaging involves irradiation of the specimen with monochromatic light and capture of intensified images on a high-speed digital CCD camera. The cameras are software-controlled, acquiring digital video images at a high frame-rate. These images are analyzed in a computer workstation following data acquisition.

### Mouse model

We use the cremaster muscle model to visualize the microcirculation in mice as described [6]. Briefly, the animal is anesthetized with an intraperitoneal injection of ketamine (125 mg kg<sup>-1</sup>), xylazine (12.5 mg kg<sup>-1</sup>), and atropine sulfate (0.25 mg kg<sup>-1</sup>), and the jugular vein is exposed under a dissecting microscope and cannulated. For some experiments, the femoral vein is used to introduce reagents into the circulation. When blood pressure is monitored continuously, a transducer is associated with the carotid artery. The trachea is always cannulated to facilitate spontaneous respiration. The animal is then placed on a custom-designed Plexiglas tray, and the cremaster muscle is exteriorized through an incision in the scrotum. After removal of the connective tissue, the muscle is pinned across a coverslip mounted within the tray. The muscle preparation is superfused throughout the experiment with preheated (37 °C) bicarbonate-buffered saline, aerated with 5% CO<sub>2</sub>/95% N<sub>2</sub> and kept warm on a heated water blanket. The animal is then moved to the microscope stage. Buffer superfusion is restarted immediately upon repositioning of the animal onto the microscope stage, and the meniscus generated by the buffer is used to immerse the lens of the microscope objective. The procedure described typically requires 5–7 min. Anesthesia is maintained with Nembutal (50 mg kg<sup>-1</sup>) injected through the jugular vein as needed. The same access is also used for the injection of antibodies, fluorochromes, cells, etc.

### Cell and protein labeling

Several approaches can be used to visualize the various components of a thrombus in the microcirculation. Each has advantages and disadvantages. The choice of the wavelength of the fluorochrome depends on the specific experimental design and must take into consideration background tissue autofluorescence, which is maximal at about 500 nm, and the

presence of other fluorochromes so that crossover, i.e. ‘bleeding’ of the signal generated by one channel into another, can be minimized or eliminated. When only two fluorescent labels are present, the use of Alexa 350 or 488 and Alexa 660 usually represents the best choice; when a third label is introduced, we use Alexa 350, Alexa 488 and either Alexa 660 or Cy5 (All from Molecular Probes, Eugene, OR, USA). Since Alexa 567 is excited by irradiation at 488 nm, we never use Alexa 488 (or fluorescein) with Alexa 567 (or rhodamine). Since the excitation spectrum of Alexa 640, Alexa 660 and Cy5 are broad, one has to consider that excitation of fluorochromes at lower wavelength may also excite fluorochromes with excitation maxima at higher wavelengths.

### Purified proteins

Purified proteins are labeled *in vitro* with the optimal fluorochromes, assayed *in vitro* for biological activity, and then re-infused into the mouse circulation via the jugular catheter. This requires use of commercially available proteins or necessitates purification of the critical protein, ideally from mouse tissue. Conjugation of the protein with a fluorochrome employs standard chemistry and is carried out using the fluorochrome manufacturer’s instructions. Proper analysis, however, includes examination by SDS gel electrophoresis to assure protein migration that is identical or nearly identical to the native, unlabeled protein; quantitation of fluorescence and calculation of the average number of fluorochromes per protein molecule; and assay of the protein for biological activity, either enzyme assay, binding assay, etc. to demonstrate that the labeling procedure did not impair functional activity. The fluorochrome-conjugated protein is infused into the mouse circulation via the jugular catheter. It is paramount that this labeled protein is functionally equivalent to the unlabeled protein in the mouse plasma, and neither inhibits nor enhances the activity of the native protein. In order to realize the fluorescence intensity necessary for imaging, the amount of protein infused must be significant relative to the amount of native protein. For example, when we directly label fibrinogen with Alexa fluoros, we infuse sufficient amounts of labeled fibrinogen so that 10–20% of the total plasma fibrinogen in the circulation is the labeled fibrinogen.

### Purified cells

Blood is obtained by cardiac puncture or carotid cannulation and collected in acid–citrate–dextrose buffer. Leukocytes are isolated by centrifugation. After centrifugation to obtain platelet-rich plasma, platelets are further purified by gel filtration. Cells are then labeled *in vitro* with a fluorochrome. Handling of cells during isolation can potentially perturb cell function, and this is especially true when working with platelets. Specifically, *in vitro* platelet activation can confound experiments in which labeled platelets are infused back into the circulation in an activated form. When platelets are labeled, platelet suspensions containing 3 × 10<sup>7</sup> platelets mL<sup>-1</sup> are incubated with calcein acetoxymethyl ester (0.5 mg mL<sup>-1</sup>; Molecular Probes, Eugene,

OR, USA) for 25 min at room temperature. Once hydrolyzed inside the cell, this compound becomes fluorescent and hydrophilic, a characteristic that traps it inside the cell. This method is particularly useful when platelets from one animal with a specific genotype are injected into an animal with a different genotype. For example, P-selectin<sup>+/+</sup> platelets can be injected into a P-selectin<sup>-/-</sup> mouse to investigate the role of platelet-derived P-selectin as opposed to endothelial cell-derived P-selectin. These platelets are infused into the mouse via the jugular catheter. Depending upon the particular experiment to be performed, the labeled platelets represent 0.5–10% of the total circulating platelets. Calcein AM can also be used to label other blood cells.

#### *Antibody labeling: direct*

Antibodies can be directly labeled with various fluorochromes, and these antibodies infused for *in vivo* labeling of target antigens. We prefer the Alexa series of fluorochromes (Molecular Probes), which offer the advantage of a low rate of photobleaching. Antibodies are labeled by incubating purified antibody with the label, followed by gel filtration to separate the labeled antibody, which elutes in the void volume, from the excess label. In some cases, labeled antibodies are available commercially, although this limits the choice of both labels and antibodies. Direct labeling of primary antibody reduces the number of proteins to be infused and therefore the non-specific 'trapping' of molecules within the thrombus. It also reduces the complexity of interpretation, where there could be concern about cross-species binding of secondary antibodies. However, in controlling the experiment by comparison of the signal generated by the relevant antibody with that generated by a non-immune control, it is crucial that every antibody has an isotype-matched control if the primary antibody is monoclonal, or a non-immune IgG if the primary antibody is polyclonal, with exactly the same fluorochrome : protein ratio, i.e. molar fluorescence yield. While this is in principle true for all immunochemical assays, it appears to be particularly relevant in this *in vivo* model in which non-specific binding cannot be overcome by more stringent washing steps, for example.

The use of F(ab')<sub>2</sub> fragments, obtained by pepsin digestion of the whole IgG molecule followed by affinity chromatography using a Protein A–Sepharose column to retain the Fc fragments, is sometimes preferred to reduce the toxic effects of the antibody or to eliminate the potential of antibody–Fc receptor interaction on cell surfaces. Platelet labeling can be achieved by injecting a fluorescently labeled Fab or F(ab')<sub>2</sub> fragment of a rat monoclonal antibody directed against the membrane glycoprotein IIb (CD41). We generally observe that upwards of 70% of platelets are labeled *in vivo*, a value determined by flow cytometry of blood platelets removed from the mouse circulation.

#### *Antibody labeling: indirect*

Alternatively, labeled anti-immunoglobulin antibodies can be used for indirect immunofluorescence where the target primary antibody is detected *in vivo* with a secondary, fluorescently

labeled antibody. An advantage of this approach is that detection in these experiments using the primary specific antibody and the primary control antibody is with the same secondary, labeled antibody.

### **Experimental thrombus generation**

Several methods have been proposed to induce thrombus formation in mice [2]. In our models, we use a nitrogen dye laser to injure endothelial cells [5]. The site of the vessel wall to be injured is established and several images of the field are captured. The laser beam is then aimed at the endothelial cell monolayer through a crosshair in the ocular and bursts of laser light for a predefined time interval are delivered. The power and frequency of these bursts is empirically determined and depends on the thickness of the tissues and on the desired size of the thrombus. For most of our experiments, we have generated sufficiently accurate data by capturing a few images of the site to be injured prior to ablation, ablating while looking through the ocular lenses of the microscope and then rapidly switching to the camera view while initiating image capture. In this method, proper barrier filters must be in place when ablating to avoid eye injury. We have found the thrombi generated by this method to be more consistent in size than those created by the alternative method described below. Image capture generally begins approximately 7 s after the first signs of thrombus generation are noted. This is the time needed to change emission filters, to alter the camera view and to initiate data capture. We have found an alternative method to be ideal: to begin digital image capture prior to ablation, to continue to capture images while effecting vessel wall injury and to continuously capture images during thrombus formation. However, in practice, this can be difficult, but with experience comes skill in predictably generating a thrombus. Care must be taken to assure that the emission filter being used absorbs light at the frequency of the ablation laser so as to avoid stray reflections that might otherwise damage the intensifier or camera. This method necessitates that the laser be targeted while looking at the computer screen rather than through the microscope oculars, and the software must support real-time video imaging directed to a monitor. Furthermore, the time lag between the target's actual position due to animal movements and its image on the screen makes successful thrombus formation more difficult. Thrombi can be generated both in venules and arterioles. The number of thrombi that can be generated in a single experiment varies depending on the anatomy of the vessel tree in the specific mouse preparation. We routinely generate as many as 10 arteriolar thrombi over the course of a 60–90-min experiment, moving upstream along the vessels.

### **Intravital microscopic imaging**

Our system was developed around an Olympus AX70 microscope with a trinocular head (Olympus America, Inc., Melville, NY, USA). Although the microscope has a full set of objectives, the intravital microscopy applications described here require

mostly a 40 $\times$  and a 60 $\times$  water immersion lens (LUMPlanFI/IR), with numerical apertures of 0.80 and 0.90, respectively. Transmitted light under the specimen is delivered through a shutter (Uniblitz VS25, Vincent Associates, Rochester, NY, USA) with an electromagnetic actuator that can be operated manually (for example during thrombus generation), or through computer control during image acquisition. In this latter case, the brightfield light can be shuttered on and off to allow brightfield image capture during fluorescent illumination. During widefield microscopy, fluorescent illumination is provided by a 175-W xenon lamp that can supply light from 350 nm through 700 nm. In contrast to a mercury lamp, the xenon lamp provides similar intensity across the excitation spectrum. The excitation beam is controlled by a high-speed wavelength changer (DG-4, Sutter Instrument Company, Novato, CA, USA) that allows switching of the beam position via an electrogalvanometer-controlled mirror to pass through, in sequence, any of four positions, each with a specific excitation filter. Switching from one filter to the next is computer-controlled and is effected in time intervals as short as 1.2 ms. In our instrument, the DG-4 wavelength changer is equipped with excitation filters (360 nm, 480 nm and 590 nm; Chroma, Brattleboro, VT, USA) matched to a triple band pass dichroic emission filter (DAPI/FITC/Cy5; Chroma) in the microscope. These components allow near-simultaneous collection of images in up to three fluorescence channels and a brightfield channel.

For confocal microscopy, we use a Yokogawa CSU-10 confocal scanner (distributed as the PerkinElmer UltraView) based on Nipkow disk technology. For colocalization experiments, confocal microscopy as opposed to widefield microscopy is invaluable for image analysis and quantitation. However, although out-of-focus haze can be eliminated by confocal microscopy, the Nipkow disk and short exposure times required for real-time image acquisition greatly limit light, thus requiring light amplification with an intensifier. The resulting loss of resolution degrades the image but allows obtaining optical sections. This confocal scanner uses the same pinholes for entrance and exit light beams but is also equipped with a second rotating disk that contains approximately 20 000 pinholes, each with a microlens. The disks rotate together at 1800 r.p.m. so that the light beams raster-scan the specimen. This technology allows the microscope to capture, in theory, up to 360 frames  $s^{-1}$ . In contrast, standard point-scanning confocal microscopes have a single pinhole and take about 0.5–1 s to acquire an image. An argon–krypton three-line laser (Melles Griot, Carlsbad, CA) provides the fluorescent light for confocal microscopy, with excitation at 488 nm, 568 nm, and 647 nm. A filter wheel (Lambda L-10, Sutter Instrument Company, Novato, CA, USA) is mounted on the excitation source to enable delivery of monochromatic light. The microscope objective is mounted on a piezoelectric driver (Physiks Instrumente International, Waldbronn, Germany), which is controlled by the computer and which allows changes in the focal plane as rapidly as every 20 ms with movements as small as 0.1  $\mu\text{m}$  in the  $z$  axis.

To generate laser-induced thrombi, the system is fitted with a nitrogen ablation laser (MicroPoint, Photonic Instruments, St.

Charles, IL, USA) which is introduced via the epi-illumination port and is focused on the specimen through the microscope objectives. The output of the laser is at 337 nm but is subsequently tuned through a dye cell. We routinely use coumarin as dye, which emits at 440 nm. The laser delivers 4-nsec energy pulses, at typically 3 pulses  $s^{-1}$ , over a surface approximately 1  $\mu\text{m}$  in diameter; the energy of the pulses can be controlled by the operator. The laser beam must be periodically aligned with the crosshair by placing a coated slide onto the stage, checking where the beam causes the removal of a small area of the coating relative to the crosshair, and adjusting the alignment.

Our microscope is equipped with a motorized stage (ProScan 101, Prior Scientific, Cambridge, UK) specifically modified to accommodate our sample tray. The stage, which can be operated either via a manual joystick or through coordinates introduced into the computer, allows precise and reproducible movement of the animal preparation.

The central part of the trinocular stand is connected to a 12-bit CCD videocamera through a Gen III intensifier (Videoscope, Sterling VA, USA). The intensifier amplifies the signal that reaches the CCD chip, thus allowing shorter exposures for the same amount of available light. This increases the temporal resolution of the images, albeit at the expense of spatial resolution. The gain of the intensifier can be adjusted and is usually kept at the minimum value that allows sufficient time resolution. A higher intensifier gain significantly increases noise during image acquisition. Although Fourier transform and deconvolution programs are available to improve signal-to-noise ratios, we do not use such programs at the present time. We currently use two CCD cameras [1]: a high-resolution camera (CoolSnap HQ, Roper Scientific, Tucson AZ) which captures images in 1390  $\times$  1024 format; this camera has a high readout rate and pixel dimensions of 6.6  $\mu\text{m}$   $\times$  6.6  $\mu\text{m}$  [2]; a high-speed camera (Sensicam, Cooke Corporation, Auburn Hill, MI) with a resolution of 640  $\times$  480 and pixel dimensions of 9.9  $\mu\text{m}$ ; while this latter camera has a lower spatial resolution, its smaller format allows a faster frame rate. Without binning, the Sensicam can operate at frame rates of 30 images  $s^{-1}$  and the CoolSnap HQ can operate at frame rates of 10 images  $s^{-1}$  during capture of a fluorescent image in a single channel. In order to increase the frame rate, the image acquisition software permits binning, i.e. the combination of signal from 4 (2  $\times$  2 binning) or 16 (4  $\times$  4 binning) adjacent pixels. Again, this combines light in adjacent pixels at the expense of resolution. Binning also dramatically reduces the file size for computer storage. We have found that 2  $\times$  2 binning with the high-speed camera, while keeping the light requirement low enough for most applications, still allows us to record images with an acceptable resolution and represents an optimal compromise for most of our experiments. A schematic representation of the microscope and its components are shown in Fig. 1.

The use of digital cameras has numerous benefits, providing the potential to do quantitative two-dimensional fluorescence experiments. Optical three-dimensional images can be generated, volumes determined and intensity of fluorochromes measured as a function of time, for example.

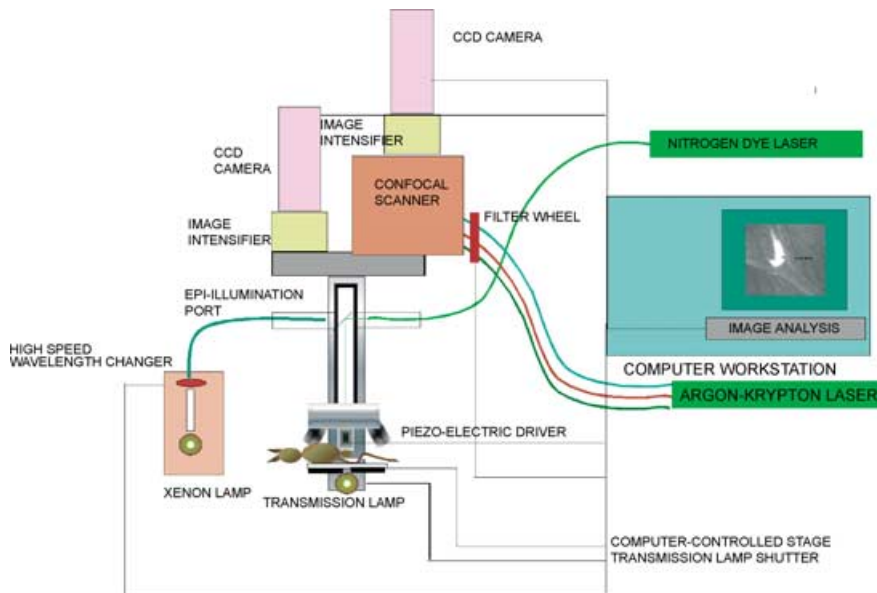


**Fig. 1.** Schematic diagram of the design of the confocal and widefield instrument for intravital microscopic imaging (modified from Falati *et al.* Nat. Med. [7]).

### Video acquisition

The images captured by the CCD cameras are transferred to the random access memory of the computer. The Dell workstation currently in use has dual 1 GHz processors, 1.5 GB of RAM, two SCSI hard drives (18 GB and 73 GB) and a Nvidia video card, and allows real-time recording of the data while connected online to the CCD cameras. A second offline workstation with similar configuration is used exclusively for image analysis so as not to interfere with data collection. Imaging software (Slidebook, Intelligent Imaging Innovations, Denver, CO, USA) is used to control and coordinate the hardware components (such as the brightfield shutter, the high-speed wavelength changer, the piezoelectric driver, the CCD camera, image acquisition channel, etc.) during image acquisition and is also used for image analysis.

### Digital video analysis

For each frame, the software provides a graphical representation (histogram) of the dynamic range of intensities within the image. Since images are captured at a 12-bit depth,  $2^{12}$  (= 4096) levels of intensity are available. The histogram presents the number of pixels ( $y$  axis) at each level of intensity ( $x$  axis). In order to differentiate subtle changes in intensity, it is important to take advantage of the full dynamic range. This requires changing the amount of light that reaches the camera, which in turn is obtained by changing light intensity, the intensifier gain, exposure time and binning. If too much light reaches the CCD camera, all pixels with an intensity above 4096 will be recorded as equal; if not enough light is available, some pixels will not be distinguishable from background noise due to autofluorescence. In a typical experiment, after the first thrombus is generated, several short videos are recorded, with changes to the above mentioned parameters until the optimal combina-

tion is obtained. If more than one fluorochrome is used, light intensity and exposure time can be optimized for each wavelength, while binning and intensifier gain must be kept constant throughout the experiment. In addition, if more than one fluorochrome is used, crossover from one channel to the other must be minimized or eliminated.

Many of our experiments involve the comparison of signals generated by specific antibodies with those generated by isotype-matched control antibodies or non-immune IgG when polyclonal antibodies are used. For the initial experiment in a series, a non-immune isotype-matched antibody, labeled by identical methods as the specific antibody, is injected, and a thrombus is generated. The intensifier gain, exposure time and binning are adjusted to minimize or eliminate the signal given by non-specific binding and background fluorescence of the non-immune antibody and mouse tissue. These settings are then used in an experiment using the specific antibody. The amount of specific antibody used must be empirically determined by titrating antibody into the animal until an adequate signal is observed. This often necessitates that the control experiment be redone using the newly determined antibody concentration. The process may be iterated several times before the ideal conditions are found. These conditions include short exposure times in each fluorescence channel to allow for good temporal resolution and a wide dynamic range. The settings thus determined are then maintained for all the experiments in a series. The image intensifier requires about 1 h of warmup before any readings are taken since intraexperiment readings can vary by as much as 20% if this device is not warmed up.

More often than not, the optimized settings still are associated with some small signal observed in the control experiments. This has necessitated the development of a method to account for background signal. As we work with living tissue, there is movement due to blood pressure pulsations, small muscle contractions, and the vessel reacting to the heat from



ablation. In addition, the background from the signal detected in thrombi with non-immune isotype matched controls is determined from an entirely different preparation, not to mention that every thrombus is different in size, shape and kinetics of growth. Thus, we cannot subtract a background field (reference) from an experimental field (sample). To deal with this issue, we use the gray-scale histogram. Looking at histograms for the non-immune control antibodies, we establish a threshold: the cut-off value below which  $\geq 95\%$  of the signal falls. Applying this threshold when analyzing the data from the experimental thrombi, we determine how much signal is above the background signal from the controls. We have found this method to

yield satisfactory results, especially if the prethrombus histograms in both experimental and control fields are similar in profile.

### Thrombus formation

To compare the kinetics and localization of platelets, tissue factor and fibrin in the thrombus in a living mouse, we performed intravital four-channel widefield fluorescence and brightfield imaging (Fig. 2) [7]. At 0 s, the initial image immediately after injury shows minimal fluorescence. Subsequently, platelets accumulate on the vessel wall. Tissue factor is also

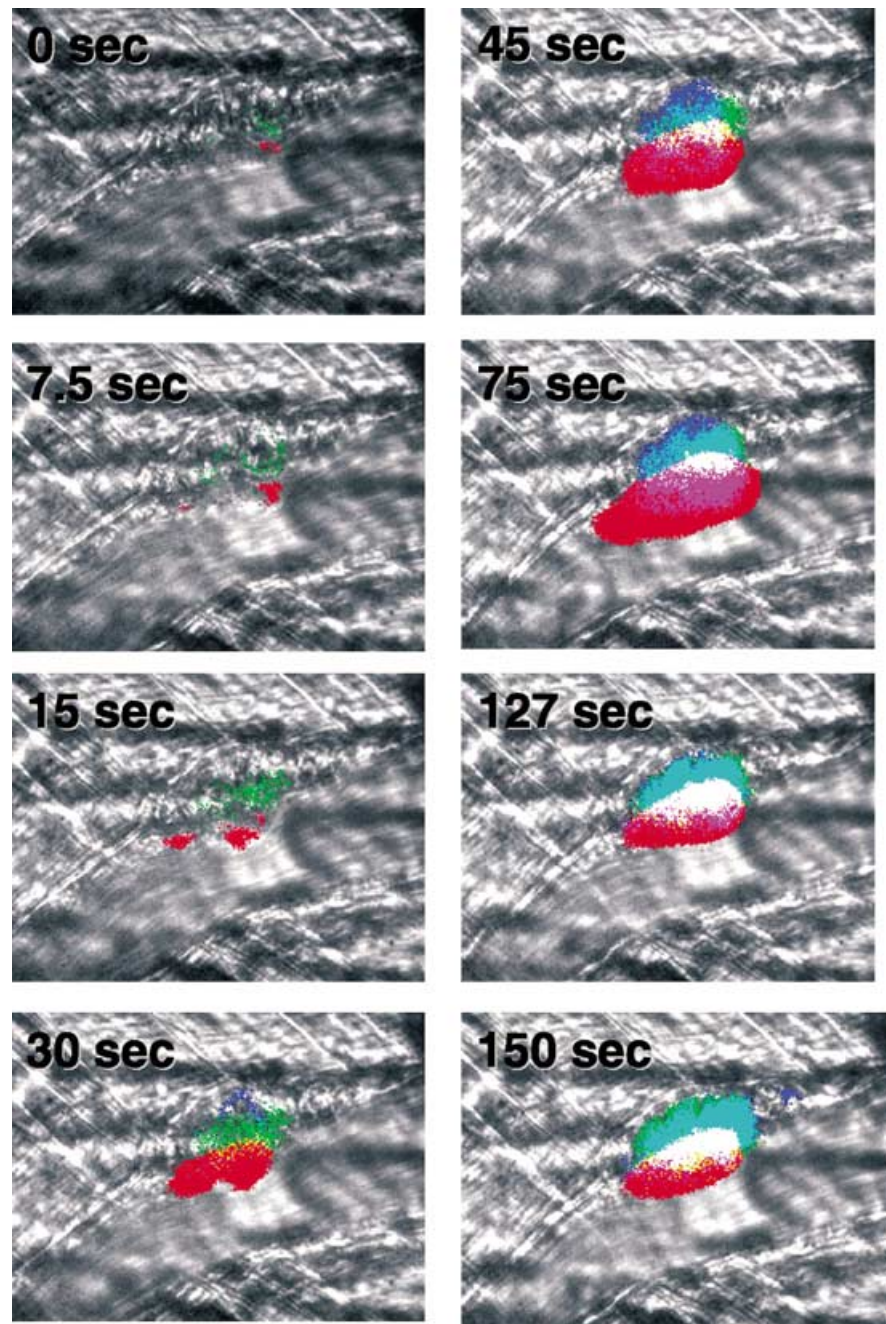


**Fig. 2.** Intravital widefield imaging of platelet, tissue factor, and fibrin deposition in the developing thrombus of a living wild-type mouse following endothelial injury. Blood flow is from right to left. Alexa 660-conjugated CD41 Fab fragments, Alexa 488-conjugated sheep antitissue factor antibodies, and Alexa 350-conjugated mouse antihuman fibrin antibodies were infused into the systemic circulation. Thrombus components in four separate channels were identified in pseudocolors as well as a black and white brightfield image, and a composite image generated. To simplify analysis of the composite image, the dynamic range of the intensity of each pseudocolor was minimized. Platelets (red); tissue factor (green); fibrin (blue); platelets + tissue factor (yellow); tissue factor + fibrin (turquoise); platelets + fibrin (magenta); platelets + fibrin + tissue factor (white). The time, in seconds, indicates the approximate interval from vessel wall injury to image capture. This image is available as a videoclip on <http://wip.blackwellpublishing.com/products/journals/suppmat/JTH/JTH33/JTH33sm.htm>.

observed but the signal-to-noise level is too low to be certain whether this initial signal is tissue factor-specific. With platelet thrombus expansion, the quantity of fibrin and tissue factor, particularly at the thrombus–vascular wall interface, increases. The composited four-channel image indicates that platelets are the major component of the arterial thrombus. Fibrin is localized on the vessel wall and then extends through part of the thrombus during the period examined. In these images, tissue factor is closely associated with fibrin.

### Three dimensional reconstruction of a thrombus

High-speed confocal intravital microscopy has been used to perform detailed structural analysis of the growing thrombus generated by laser-induced injury. Using a piezo-electric driver on the microscope objective lens, image ‘slices’ of 0.1–1  $\mu\text{m}$  can be obtained at a high frame rate. These slices are stacked, thus generating an optical three dimensional computer reconstruction of the thrombus (Fig. 3; video).

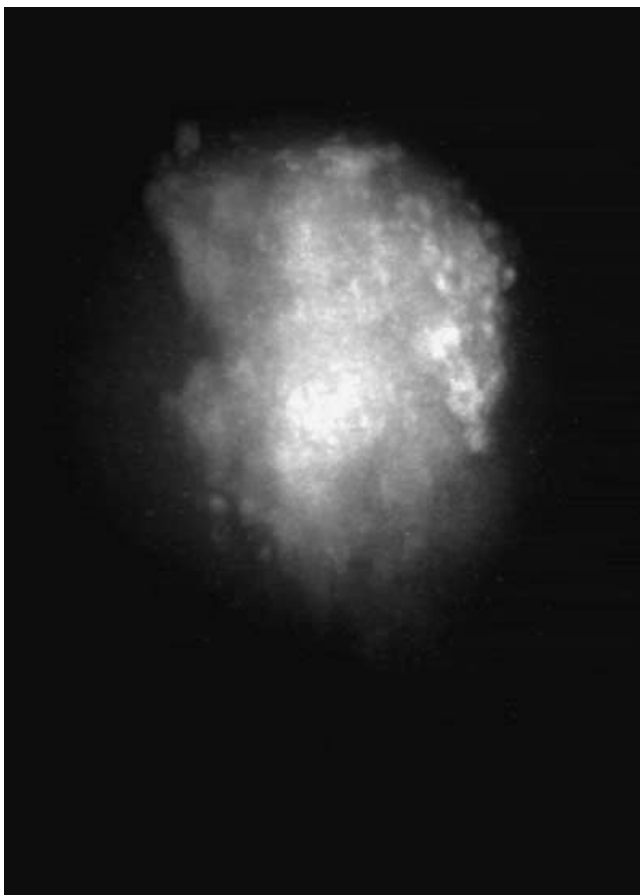


**Fig. 3.** Three-dimensional image of a thrombus. An arteriole of the cremaster muscle was injured. Images of fluorescent platelets in the thrombus were obtained as the working distances between the objective and the specimen were rapidly altered using the piezo-electric driver. At each confocal plane, a 2D image was obtained. In this experiment, confocal XY images were stacked in sequential order with the imaging software to yield a 3D image of the thrombus. This image is available as a videoclip on <http://wip.blackwellpublishing.com/products/journals/suppmat/JTH/JTH33/JTH33sm.htm>.

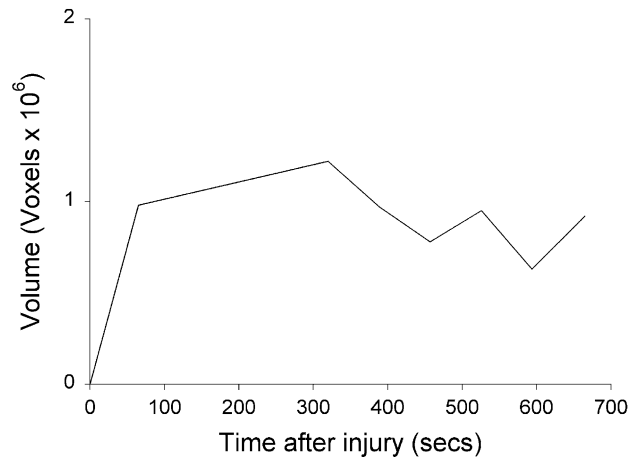


**Fig. 4.** The kinetics of *in vivo* thrombus development. Platelets were fluorescently labeled and a postcapillary venule of the cremaster muscle was injured using the laser system. Confocal images of fluorescent platelets in the thrombus were obtained sequentially using the piezo-electric driver. The resulting 2D image were stacked in sequential order with the imaging software to yield a 3D image of the thrombus. Repeated 3D thrombus imaging allowed determination of thrombus volume as a function of time. These experiments require digital confocal microscopy and cannot be performed by widefield microscopy.

### Thrombus volume determination

The volume of thrombi formed *in vivo* can be determined by confocal microscopy and image analysis. In a thrombus, a three dimensional thrombus image is obtained in which each component is labeled by a different fluorochrome. The total volume of the thrombus is obtained by image analysis. The boundary between the thrombus and the flowing blood is defined, and the thrombus surface structure rendered. Pixels included within this volume, including pixels defined by each of the fluorochromes reporting each of the thrombus components, are totaled to yield the number of ‘voxels.’ Since the dimension of a single pixel is known for a given magnification and thus the voxel volume is known, totaling of the number of voxels within a thrombus yields the thrombus volume in  $\mu\text{m}^3$ . To obtain the volume of a thrombus component, such as platelets, the number of voxels within the thrombus that are defined by the platelet-specific fluorochrome are totaled (Fig. 4).

### Thrombus embolization

The thrombi that are generated in the mouse microcirculation undergo embolization, with small segments of the thrombus breaking off and flowing downstream. To formally quantitate this phenomenon, we have established methods for detecting the image of the embolism as it floats downstream, and we can quantitate the fluorochrome in the embolism (Fig. 5; video). Using a high image capture rate of over 100 frames per second, the integrated intensity of each thromboembolus is measured as a function of time. This high capture rate is achieved using a combination of  $8 \times 8$  binning and limiting the region of interest. The region of interest is that portion of the CCD chip-capturing

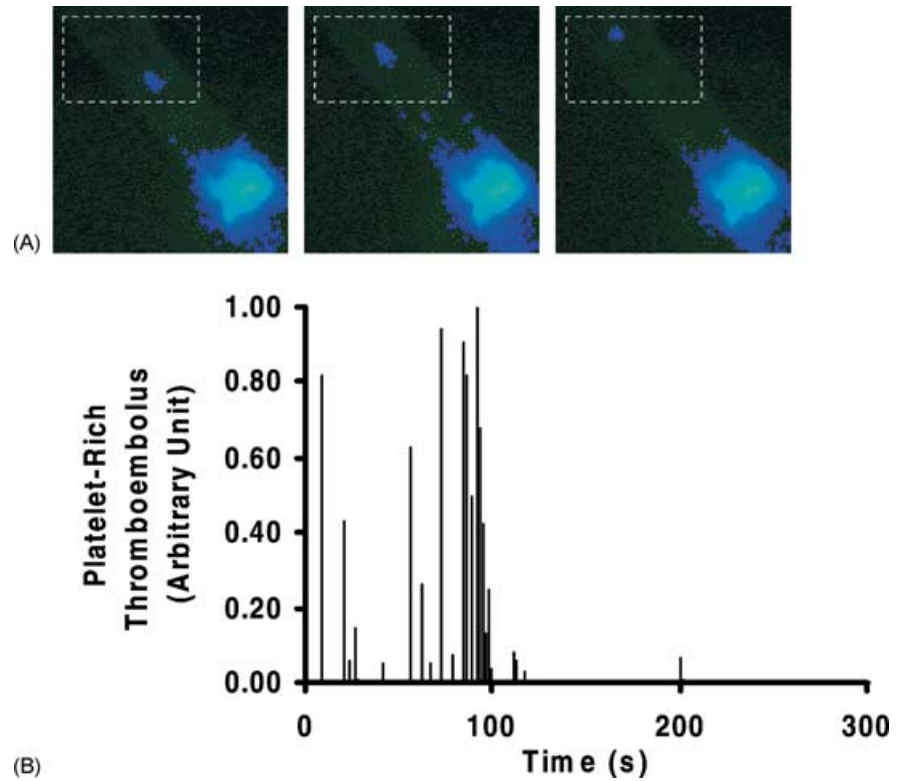


**Fig. 5.** Quantitation of thrombus microembolization during thrombus formation. The total amount of thromboemboli originating from a thrombus has been quantitated by widefield fluorescence microscopy. (A) In this series, a thromboembolus digitally recorded at 9-ms intervals is pictured in the dashed box. Thromboembolic events are captured by defining a subarray of pixels downstream of the thrombus with regard to blood flow. (B) The integrated fluorescence of thromboemboli entering the defined subarray over a period of 300 s is recorded. Each bar represents a unique thromboembolic event.

signal related to embolization. The fluorochrome in the experiment shown was associated with platelets. Multiple embolic events can be detected, and the amount of fluorochrome (proportional to the number of platelets) in each embolus is quantitated. This allows formal analysis of a series of events observed previously using analog videomicroscopy, but which could not be analyzed quantitatively and compared.

### Image analysis and data interpretation

In designing and integrating the hardware for this system, it has become abundantly clear to us that despite the complexity of the components and their interfaces with each other, experimental design and data interpretation are even more complex. Hidden under the elegant images that emerge from these experiments is the travail in design, execution, balance, and interpretation. What you see is *not* what you get! More accurately, as the sign at the School of Cinema–Television at the University of Southern California says, ‘Reality stops here’. The digital revolution, as applied to imaging, can introduce artifacts and misconceptions, and the investigator needs to be especially critical. Problems that we have encountered with our system and resolved include: (i) shuffling of channels (i.e. inappropriate assignment of specific images to specific color channels); (ii) cross-over of one fluorescent channel into another channel; (iii) image artifacts due to pixel saturation and software bugs; (iv) three-dimensional reconstructions without proper definition of the  $z$  axis and interpolation between image slices; (v) generation of fluorescent images, even in multiple colors, does not include

sufficient information for analysis and interpretation; inclusion of the brightfield background provides histologic context to the events monitored by fluorescence microscopy; (vi) unequal labeling of control and experimental antibodies; and (vii) perturbation of mouse physiology with an inhibitory antibody. Problems that arise in these types of analyses regardless of the system used include: (i) claims of colocalization in widefield images because pixels contain signal from two channels, although the source of the signals may be relatively nonadjacent in the  $z$  axis (i.e. colocalization can only be determined by confocal images); (ii) lack of a uniform definition for real-time imaging (continuous images 4–5 frames  $s^{-1}$  might serve as a provisional definition); (iii) the rate of change in tissue architecture must be slow with respect to the image-capture rate; (iv) inadequate management of background and non-specific binding; and (v) photobleaching of fluorochromes over time competes with the accurate measurement of the kinetics of concentration change of fluorescently labeled proteins or cells.

### Future directions

Using these methods, we are able to analyze the accumulation of proteins and cells that participate in thrombus formation. We are able to observe platelet recruitment, tissue factor accumulation and fibrin deposition during thrombus development, and to compare the time course of platelet and fibrin assembly into the thrombus [7]. Furthermore, we have demonstrated that tissue factor, although distributed throughout much of the growing



thrombus, is concentrated on the vessel wall–thrombus interface. In separate studies, we have shown that P-selectin, an adhesion molecule expressed by activated platelets and stimulated endothelial cells, colocalizes with platelets, indicating that platelets within the thrombus undergo activation and degranulation under our experimental conditions [8]. We have also demonstrated that tissue factor accumulation and fibrin deposition in the growing thrombus is dependent upon both P-selectin and PSGL-1 since these thrombus components are absent or nearly absent in mice lacking these adhesion molecules [9]. Numerous other *in vivo* studies, particularly those involving various genetically altered mice, are in the preliminary stages of development.

We see a number of challenges ahead. Intrinsically fluorescently labeled components, particularly those in low concentration and not optimal targets for antibody-based labeling, would be ideal. We have used green fluorescent protein-containing platelets, prepared by replacement of the Gz gene with GFP [10], as one approach to generating fluorescently tagged platelets without the use of exogenous fluorochromes. On a separate front, we are examining the antithrombotic potential of several small molecules using this thrombosis model, with special emphasis on how they contribute to diminished thrombus size [11].

To fully exploit the potential of this new system, we are working to develop quantitative assays to translate color intensity in confocal images into fluorochrome concentration. Such analysis is only possible in confocal mode since rigorous quantitation requires the summation of the thin image slices that, added together, represent the three-dimensional structure. This would allow meaningful comparison of color intensities in three channels; intensities could be converted into concentration of thrombus components. We also await improvement in CCD camera technology and intensifier technology, both of which will lead to higher resolution and faster frame-rates of image capture. In addition, improved control over the emission wavelength or filter coatings would offer improvements in color separation and the potential for introduction of an additional fluorescence channel.

## Conclusion

Direct visualization of *in vivo* processes, including thrombus formation, leukocyte rolling, and blood coagulation, offers new potential for understanding of complex biological processes such as hemostasis, thrombosis and inflammation. Coupled with novel mouse strains and murine models of human disease, opportunity exists for examining biochemical, physiologic and pathologic processes in living animals.

## Acknowledgments

We thank Dr Shinya Inoué for introducing us to the Yokagawa confocal scanner, Dr Ken Spring for helpful comments in the design of the widefield fluorescence microscope, Drs Francis Castellino and Elliot Rosen for demonstration of the laser ablation injury model, Eric Furie for extensive consultation on digital image acquisition and data storage, Drs Karl Kilborn and Ben Freiberg for continuous enhancement of *Slidebook* to meet the needs of our unique application and the faculty of the course 'Optical Microscopy & Imaging in the Biomedical Sciences' at the Marine Biological Laboratory in Woods Hole MA, USA. This work was supported by grants from the National Institutes of Health (HL51926 and HL69435). The confocal microscope was obtained with partial support from the National Institutes of Health (S10RR15680).

## References

- 1 Furie B, Furie BC. Molecular and cellular biology of blood coagulation. *N Engl J Med* 1992; **326** (12): 800–6.
- 2 Carmeliet P, Lieve M, Collen D. Mouse models of angiogenesis, arterial stenosis, atherosclerosis and hemostasis. *Cardiovascular Res* 1998; **39**: 8–33.
- 3 Inoue S, Spring KR. *Video Microscopy*. New York: Plenum Press, 1997.
- 4 Inoué S, Inoué T. Direct-View High Speed Confocal Scanner—the CSU-10. In: Matsumoto B, ed. *Biological Applications of Confocal Microscopy*, Academic Press, New York, 2002 (in press).
- 5 Rosen ED, Raymond S, Zollman A, Noria F, Sandoval-Cooper M, Shulman A *et al*. Laser-induced noninvasive vascular injury models in mice generate platelet- and coagulation-dependent thrombi. *Am J Pathol* 2001; **158**: 1613–22.
- 6 Yang J, Hirata T, Croce K, Merrill-Skoloff G, Tchernychev B, Williams E *et al*. Targeted gene disruption demonstrates that P-selectin glycoprotein ligand 1 (PSGL-1) is required for P-selectin-mediated but not E-selectin-mediated neutrophil rolling and migration. *J Exp Med* 1999; **190** (12): 1769–82.
- 7 Falati S, Gross P, Merrill-Skoloff G, Furie BC, Furie B. Real-time *in vivo* imaging of platelets, tissue factor and fibrin during arterial thrombus formation in the mouse. *Nat Med* 2002; **8**: 1175–81.
- 8 Gross PL, Furie BC, Furie B. Kinetics of platelet activation, P-selectin expression and leukocyte rolling during arterial thrombus formation. *Blood* 2002; **100** (Suppl.): 23a (Abstr.).
- 9 Falati S, Gross P, Merrill-Skoloff G, Croce K, Furie BC, Furie B. *In vivo* real time imaging of arterial thrombus formation reveals P-selectin- and PSGL-1-mediated tissue factor accumulation as a mechanism for fibrin clot generation. *Blood* 2001; **98**: 823a.
- 10 Yang J, Wu J, Kowalska M, Dalvi A, Prevost N, O'Brien P *et al*. Loss of signaling through the G protein, Gz, results in abnormal platelet activation and altered responses to psychoactive drugs. *Proc Natl Acad Sci U S A* 2000; **97**: 9984–9.
- 11 Sim DS, Merrill-Skoloff G, Furie BC, Furie B, Flaumenhaft R. Initial accumulation of platelets following vascular injury is mediated by phosphodiesterase. *Blood* 2002; **100** (Suppl.): 51a (Abstr.).